

Implement the artificial neural network concept for predicting the mechanical properties of printed polylactic acid parts

Mazin Al-Wswasi^{1*} , Weam A. Al-Khaleeli¹ , Samah A. Aufy¹

¹ Production Engineering and Metallurgy Department, University of Technology-Iraq, Iraq

* Corresponding author's e-mail: mazin.g.abdulrazzaq@uotechnology.edu.iq

ABSTRACT

Additive manufacturing (AM) is an industrial process that involves creating three-dimensional (3D) parts based on computer-aided design (CAD) models. Various methods and techniques have been developed in the recent decade to enhance this industry. This research observes the influence of 3D printing parameters using fused deposition modeling (FDM) on the uniaxial compressive strength (UCS) of polylactic acid (PLA) specimens. This is precisely to study the effects of infill density, infill pattern, and layer thickness and determine the optimal parameters. The compression test samples have been designed based on ASTM D695 standards and manufactured using a Creality Ender-5 Pro 3D printer. Then, a Taguchi design of experiments method has been used, and nine experiments have been conducted to evaluate the effects of the mentioned parameters. Also, analysis of variance (ANOVA) declared that the infill density is the most noticeable parameter with a contribution of 83.56% to the variation in UCS. On the other hands, both infill pattern and layer thickness had minimal impact. However, the ideal configuration to earn maximum UCS value has been recorded as 80% infill density, a gyroid infill pattern, and a 0.3 mm layer thickness based on ANOVA analysis. Furthermore, an artificial neural network (ANN) model has been developed to enhance predictive capabilities. This is by training a three-layer architecture with inputs of infill density, infill pattern, and layer thickness. It is confirmed by two calculation outcomes that the ANN has performed high predictive accuracy: a regression coefficient (R) of 0.9974 and slight deviation between experimental and predicted UCS values. These results show the considerable role of infill density in increasing the compressive strength, as well as approve the ANN as a trusted tool for predicting mechanical properties of 3D-printed components. This research presents profound investigation for optimizing FDM parameters to enhance the mechanical performance of 3D-printed parts.

Keywords: 3D printing, fused deposition modeling, PLA, ANOVA, artificial neural network.

INTRODUCTION

Additive manufacturing (AM), which is also described as three-dimensional (3D) printing, is a forming process produces simple and complex shapes through layer-by-layer deposition. Among many other targets, it aims to reduce material waste, improve precision, and decrease reliance on manual labor [1]. Furthermore, the key improvements in AM have concentrated on aiding the production of large structures, reducing printing defects, and improving mechanical properties. Nowadays, the latest versions of AM have participated in producing complex parts and forms, adopting it as a method for prototype and final

products in industries such as household goods, automotive, sports, and healthcare sectors [2].

There are different AM techniques, such as directed energy deposition (DED), material extrusion, material jetting, and powder bed fusion. Metals, polymers, and ceramics are the commonly used materials with these processes [3]. For instance, the FDM technique applies polymer filaments, while powder particles are used with both selective laser melting (SLM) and selective laser sintering (SLS) methods [4]. This study emphasizes the research on the FDM technique.

FDM can be considered as one of the widely used AM techniques. It is dependable for manufacturing 3D parts for both final-use parts and

under evaluation prototypes that are challenging to be manufactured with traditional methods [5]. The FDM process is achieved by depositing successive layers of extruded thermoplastic filaments to create a 3D object. Different types of filaments can be used with FDM, such as a PLA, acrylonitrile butadiene styrene (ABS), polypropylene (PP), or polyethylene (PE) [6]. However, PLA can be considered one of the most commonly used materials due to its robust mechanical characteristics, excellent printability, and sustainability [7]. Moreover, PLA can be easily processed via traditional techniques, such as extrusion, compression molding, and injection molding, as well as modern techniques like 3D printing [8].

In this field of research, several studies have proposed statistical methods for the purpose of enhancing the quality of FDM parts. The followed strategy comprises optimizing process parameters for specific performance outcomes. Brischetto and Torre [9] have worked on experimental tensile and compression tests to evaluate the mechanical properties of FDM-printed PLA specimens. The investigated properties include the linear Young's modulus, linear elastic limit stress, and ultimate tensile strength. Their study focused on recognizing the mechanical behavior under tensile and compressive states and specifying the effect of process parameters on these properties. Chandran et al. [8] have manufactured PLA specimens in two different manufacturing methods: compression molding and 3D printing. Then, the tensile properties of these specimens have been compared. The authors aimed to analyze existing knowledge regarding the mechanical properties of PLA, study the effects of manufacturing processes on these properties, and understand the impact of water absorption on its performance.

The research of Nguyen et al. [3] proposed a methodology for the purpose of optimizing the printing parameters to maximize the tensile strength of PLA specimens via genetic programming (GP) and a genetic algorithm (GA). These methods have not only succeeded in achieving optimization, for they also able to predict PLA test results. Firstly, Eureka software has been utilized to implement GP. Next, they used GP to develop a surrogate model that correlates tensile strength with key parameters. Finally, a GA has been employed to recognize the optimal printing settings, which can maximize the tensile strength of the specimens. According to the authors, the proposed model demonstrated excellent agreement with

experimental results. Fisher et al. [2] have carried out an experiment to investigate the influence of short carbon fiber reinforcement, infill orientation, and strain rate on both the tensile and compressive properties of 3D-printed specimens. It has been concluded that strain rate and print orientation significantly influence the mechanical properties of both reinforced and non-reinforced nylon. These findings can contribute improving the design and numerical modeling of 3D-printed composites.

Hamed and Abbas [10] have focused on critical process parameters to evaluate the performance of FDM performance in printing objects with maximum compressive resistance. Taguchi method has been implemented to examine infill density, outer shell width, infill pattern, and layer thickness with minimal experimental testing. The effects of these parameters have been analyzed, and a linear regression model has been applied to predict the experimental results, achieving a low error rate of 4%. Whilst, Sultana et al. [11] have analyzed how 3D printing parameters affect the mechanical properties, including tensile strength of wood filament, an industrial polylactic acid-based wood fiber composite material. The factors of this study include layer thickness, infill density, printing speed, and nozzle temperature. A Taguchi L9 orthogonal array had used to design the experiment of tensile. Whereas, the ANOVA is employed to recognize the importance of each parameter. Finally, a scanning electronic microscopy (SEM) has been used to analyze the fracture zones, cracks, voids, and fiber/matrix adhesion. Farias et al. [12] have tested the influence of 3D printing parameters on the mechanical properties under compression. The research investigated some factors such as infill patterns (hexagonal, triangular, and concentric), shapes (solid and honeycomb), and carbon nanotube (CNT) concentrations of 1.0 wt% and 2.0 wt%. The results showed that these parameters, combined with the addition of CNTs, can improve the properties of products manufactured using AM techniques.

Abdulridha et al. [13] have focused on improving the surface finish and quality of 3D-printed objects. Their study analyzed the effects of various factors such as infill overlap percentage, shell thickness, layer thickness, and the number of top and bottom layers. Both Taguchi and ANOVA have been used in designing and analyzing the experiments, respective. The results approved that the surface quality of FDM components can be enhanced through employing

a micro-stage process with low dimensional variation, combined with vapor smoothing process (VSP) treatment. Also, an optimal surface finish has been gained using dichloromethane chemical under specific parameter settings. Tunçel [14] has evaluated the effects of printing factors on Charpy impact strength. This includes infill density, raster angle, layer height, and print speed. A Taguchi L16 orthogonal array is used for experimental design, along with ANOVA, for the purpose of examining, analyzing, and optimizing the impact strength of strong PLA material manufactured using FDM. It was indicated that infill density and print speed had major effects on impact strength, with optimized parameters increasing it by 1.39%, resulting in a 38.54 kJ/m² impact strength. Later, Abdulridha et al. [15] employed PLA material in ultimate tensile and compressive strength (UTS and UCS) tests, to predict model using ANNs. The parameters of this study are (layer thickness (mm), percentage of infill density, number of top/bottom layers, shell thickness (mm), and infill overlap percentage. The study applied Taguchi design of experiments method, involving a (L25) orthogonal array in addition to a neural network (NN) technique with two layers and 15 neurones. It is showed the infill density has an important effect on UCS and UTS, with displayed results matching experimental values, providing for flexibility in ideal settings.

The mechanical properties of parts produced using FDM are influenced by the specific parameters selected during the printing process. Due to the variations in these parameters, some printed samples may exhibit poor mechanical properties. In this study, a feed-forward NN model, with a backpropagation (BP) algorithm, has been trained, tested and validated to investigate the impact of FDM parameters, which are specifically infill density, infill pattern, and layer thickness, on

the UCS of printed samples. In order to enhance the quality of printed parts, the developed system can adjust the three mentioned parameters continuously. This has been achieved by creating an ANN model with multiple inputs and outputs.

EXPERIMENTAL WORK

The proposed methodology starts with designing and manufacturing standardized compression test specimens using a 3D printer. The consistency of the sample dimensions and geometry must be guaranteed. Then, the compression ability of the 3D-printed specimens is evaluated through mechanical testing. After completing the test phase, a statistical analysis using ANOVA is achieved to assess the significance of the 3D printing parameters on the mechanical properties. Finally, a neural network is employed to further analyze the influences of these factors and recognize optimized settings. The details of each phase are demonstrated b experiment and practical application. in the following sections.

Material and specimen

The compression test specimens have been designed according to the ASTM D695 standard. This has been achieved using the SOLIDWORKS 2022 platform for the purpose of creating 3D models of the specimens as computer-aided design (CAD) files. Next, these 3D models are converted into standard triangle language (STL) format, which is compatible with many machines and systems. Figure 1 a and b show a 3D model of specimen in SOLIDWORKS and its STL file, respectively. After generating the STL file, the 3D model is sliced into thin layers. Figures 2a, 2b, and 2c show three different patterns cubic, gyroid, and concentric,

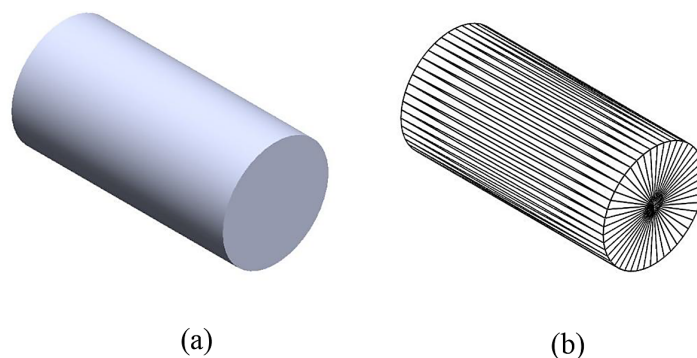


Figure 1. 3D model of specimen a) SOLIDWORKS and b) STL file

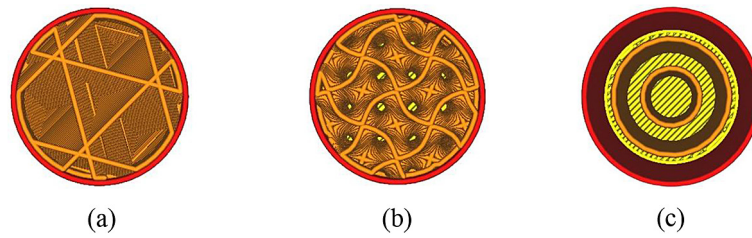


Figure 2. The top view of three different patterns a) cubic, b) gyroid, and c) concentric

respectively. Finally, Ultimaker Cura 5.6.0 software is used to configure the printing process parameters and generate the G-Code for the printer.

Regarding the printing phase, yellow PLA is chosen as the material of this study not only for sustainable issues, for it also performs better in cavities [16]. The PLA filament has a diameter 1.75 ± 0.05 mm, a melting point of 195–235 °C, density of 1.25 g/cm³, an impact strength of 12 kJ/m², a flexural strength of 48–110 MPa, a tensile strength of 61–66 MPa, a fracture elongation of 0.7%, and a tensile modulus of 2.7–16 GPa.

After preparing the G-code and determining the parameters of the machine, the Creality Ender-5 Pro FDM printer with 0.4 mm nozzle diameter was selected to manufacture the specimens. Figure 3 shows the Creality Ender-5 Pro



Figure 3. Creality Ender-5 Pro 3D printer

3D printer. The printer starts hotly extruding the PLA filament via its circular nozzle. The moving printing head deposits the extruded filament in a user-specified pattern onto a heated metallic substrate. After a particular layer is finished, the printing head is raised to deposit the next layer. Whilst the layer thickness, deposition velocity, extrusion temperature, and PLA filament feeding rate are all manually adjustable by the user, the printer automatically calculates the distance between successive filament depositions. This is based on user-controlled parameters and volume conservation considerations [17].

Parameter and techniques

Most, if not all, the 3D printers have variety of parameters. Each effect on the quality, strength, and efficiency of the printed objects. The parameters include infill density (20%, 50%, 80%), infill pattern (Cubic, Gyroid, Concentric), and layer thickness (0.1 mm, 0.2 mm, 0.3 mm) as mentioned in Table 1. However, the printing temperature, build plate temperature, and printing speed were constant as 200 °C, 50 °C, and 80 mm/sec, respectively.

An influential, straightforward, and systematic technique is produced through the design of experiments utilizing the Taguchi method for identifying the ideal parameters in the production process. The three levels of variation for each parameter are used in conjunction with the Taguchi method to measure the performance characteristics that deviate from the required values, utilizing the signal-to-noise (S/N) ratio.

Table 1. The selected process parameters in this study

Variables	Levels			Units
	1	2	3	
Infill density	20	50	80	%
Infill pattern	Cubic	Gyroid	Concentric	-
Layer thickness	0.1	0.2	0.3	mm

Consequently, nine specimens have been designed, printed, and experienced. In order to maximize compressive strength, the higher-the-better criteria should be selected. Equations 1 can be used to represent the S/N ratio for the mentioned performance characteristic:

$$\frac{S}{N} = -10 \log \left(\frac{1}{n} \sum_{i=1}^n \frac{1}{y_i^2} \right) \quad (1)$$

where: n – measurements total number, y_i – the value of the characteristics that were measured.

All the nine experiments have been accomplished using a WDW- 200E computer-controlled electronic universal testing machine with a cross-head velocity of 1.5 mm/min. This has been conducted in the Department of Production Engineering and Metallurgy. Figure 4 a and b show the controlled testing machine and one of the specimens during the experiment, respectively.

The next step includes the calculation of stress for each specimen based on original dimensions from the CAD model. Equation 2 can be used to determine UCS for each PLA test specimen according to the necessary information:

$$\sigma = \frac{F}{A} \quad (2)$$

where: σ – the tensile and compressive stress in (N/mm²), F – the applied force in (N), A – the cross-sectional area of the printed specimen in (mm²).

Artificial neural network

After completing the mechanical experiments, an ANN tool is utilized for learning-based information processing in pattern recognition, data classification, and application-based problems.

The neural network involves three layers: input, hidden, and output. Starting with the input layer, it consists of three input neurons: infill density (%), infill pattern, and layer thickness (mm). Since nine experiments have been conducted, the dimensions of the input matrix are 3×9 . The hidden layer depends on the inputs and the weights assigned to their components. These weights can be adjusted, as this research employs the Hebbian learning rule in the neural network (NN) model [18]. In fact, the Hebbian learning rule can detect and leverage the input correlations. The process begins when multiple sets of input data are fed into the network. The system then modifies the weight values based on errors generated by comparing the expected results with the actual outcomes [15].

Regarding the output layer, it is assigned one output neuron that represents the UCS values from the experimental calculations, formatted as a 1×9 matrix. As seen in Figure 5, the neural network architecture.

RESULTS AND DISCUSSION

Analysis the results

The mechanical characteristics, represented by UCS, of nine FDM specimens have been measured, and the results are shown in Table 2. Then, the data are analyzed with Minitab 17 to help in predicting the optimal parameter levels. Also, a statistical ANOVA is used to determine which parameters have a significant impact on performance and their relationships.

The experimental data presented in Table 2 illustrate the relationship between the infill density, infill pattern, and layer thickness along with the UCS of the material. The findings demonstrate a

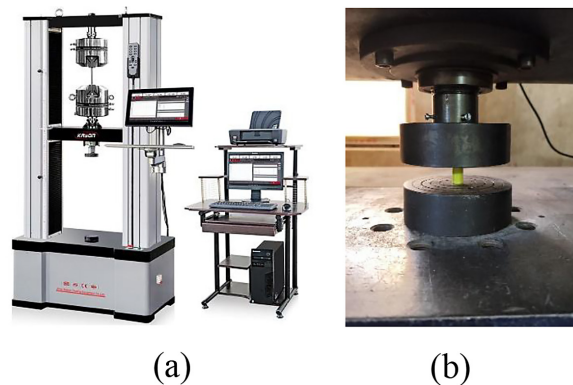


Figure 4. Compression test a) WDW-200E computer-controlled electronic universal testing machine and b) a specimen

Table 2. Results of the experimental work

No.	Infill density (%)	Infill pattern	Layer thickness (mm)	Stress (UCS)
1	20	Cubic	0.1	36.438
2	20	Gyroid	0.2	37.133
3	20	Concentric	0.3	39.406
4	50	Cubic	0.2	37.322
5	50	Gyroid	0.3	47.363
6	50	Concentric	0.1	43.574
7	80	Cubic	0.3	52.858
8	80	Gyroid	0.1	56.268
9	80	Concentric	0.2	54.878

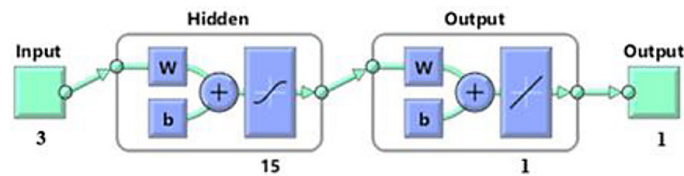


Figure 5. An illustration of the employed neural network architecture

clear trend in which infill density emerges as the most influential parameter, significantly affecting the UCS values. It takes only a glance to notice that the low infill density of 20% results in the lowest UCS values across all infill patterns and layer thicknesses, with the minimum recorded at 36.438 MPa for the cubic pattern and a layer thickness of 0.1 mm. As the infill density increases to 50%, there is a noticeable improvement in UCS values, such as 47.363 MPa for the gyroid pattern with a layer thickness of 0.3 mm. At the highest infill density of 80%, the UCS reaches its maximum, with a peak value of 56.268 MPa observed for the gyroid pattern with a layer thickness of 0.1 mm. This trend aligns with the ANOVA results, which indicate that infill density contributes 83.56% to the variation in UCS, making it the most significant factor.

Regarding the infill pattern, it also plays a crucial role in enhancing UCS, albeit to a lesser extent than infill density. However, among the three mentioned patterns, the gyroid consistently achieves the highest UCS values. This is in particular at higher infill densities. For example, at the infill density of 80%, the gyroid pattern records 56.268 MPa when having 0.1 mm layer thickness, outperforming both the concentric and cubic patterns which record (54.878 MPa) and (52.858 MPa), respectively. This means that the gyroid pattern gives superior load distribution and structural integrity in comparison with the

other patterns because it reduces stress concentration points which results in better mechanical performance. Hence, it enhances the mechanical performance while improving the strength-related capabilities and energy dissipation, as well as the layer deformation intensity, which decreases the possibility of sudden fractures. Furthermore, the layer thickness has a more subtle impact on UCS in comparison with infill density and infill pattern. Also, the thinner layers (e.g., 0.1 mm) can slightly improve UCS values; however, the overall variation caused by layer thickness is relatively minor. For instance, at infill density of 80%, the UCS values for the gyroid pattern decrease merely from 56.268 MPa at 0.1 mm to lower values at thicker layers. The ANOVA results further confirm that layer thickness contributes only 0.36% to the variation in UCS, making it the least significant parameter.

According to ANOVA analysis, the optimal combination to maximize UCS is achieved with 80% infill density, gyroid infill pattern, and 0.3 mm layer thickness, as highlighted in the results. These findings confirm the importance of selecting appropriate parameter combinations to enhance the mechanical performance of 3D-printed components, particularly for applications requiring high compressive strength. The dominance of infill density underscores its critical role in determining the structural integrity of the printed material. Table 3 presents the main attributes and interactions for

UCS that were determined using an ANOVA based on the experimental data in Table 2.

The conjunction between the ANOVA results from Table 3 with Main Effects Plot diagram Figure 6, provides a clear understanding of how the three selected factors influence the UCS of the printed structure. It has been shown that the most significant factor affecting UCS is the infill density, as evidenced by both the steep upward trend in the plot and its dominant contribution of 83.56% to the variation of UCS in the ANOVA table. The UCS increases significantly as the infill density rises from 20% to 80%, highlighting the direct correlation between the amount of material within the structure and its ability to resist compressive forces. This trend underscores that higher infill density enhances the internal structure’s load-bearing capacity, leading to a more robust component. The statistical significance of this parameter can be recognized by its low P-value (0.004) in the ANOVA results, affirming that infill density should be prioritized when designing for strength.

In contrast, the infill pattern shows minimal influence on UCS, as seen from the nearly flat trend in the plot. While there is a slight improvement in UCS for the Gyroid pattern compared to

Concentric and Cubic patterns, the variations are marginal. This aligns with the ANOVA results, where the infill pattern contributed only 7.16% to the total variation in UCS and had a high P-value of 0.307, indicating statistical insignificance. These results suggest that the choice of infill pattern does not substantially impact compressive strength, allowing flexibility in selecting patterns based on other factors such as material usage or aesthetic considerations. In addition, the layer thickness shows a minimal effect on UCS, with the plot indicating a slight increase in strength as the thickness changes from 0.1 mm to 0.3 mm. However, the trend is nearly flat, reflecting the low contribution of layer thickness (0.36%) in the ANOVA table. The high P-value (0.709) further confirms that this factor is statistically insignificant in influencing UCS. This indicates that layer thickness can be adjusted to optimize other parameters, such as printing time or resolution, without significantly compromising the compressive strength. Table 4 highlights the optimal parameter levels for achieving the maximum uniaxial compressive strength (UCS) along with their significance.

Table 3. ANOVA for UCS results

Source	DF	Adj SS	Adj MS	F-Value	P-Value	% contribution
Infill density	1	433.946	433.946	37.49	0.004	83.559
Infill pattern	2	37.211	18.606	1.61	0.307	7.165
Layer thickness	1	1.867	1.867	0.16	0.709	0.360
Error	4	46.304	11.576			8.916
Total	8	519.328				100

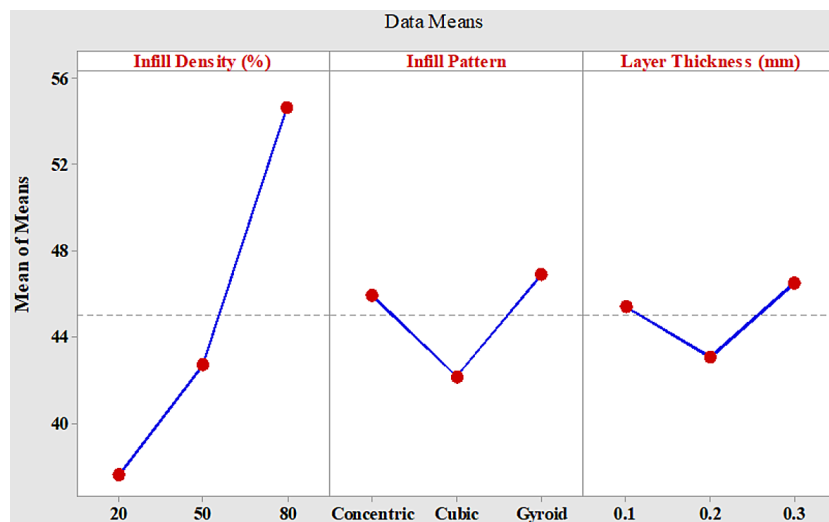


Figure 6. Main effect plot for ultimate compressive strength

Table 4. Optimum level and the significant for each parameter

Parameters	Optimized UCS
Infill density (%)	80%
Infill pattern	Gyroid
Layer thickness (mm)	0.3
Significant	Infill density (%)

Results of the developed ANN

This study employs ANN to predict results and compare them with data from actual experiments, which are also used to train the neural network. The data of the model are divided into three groups (70% training, 15% validation, 15% testing). Table 5 displays an average output response observation. Figure 7 illustrates the performance of the neural network model in terms of mean squared error (MSE) across training, validation, and testing datasets over epochs. The best

Table 5. The output response observation

Network configuration	3 – 15 – 1
The transfer function type	Trainlm
Number of epochs	100
The learning rate factor (α)	0.001
Size of neuron	15
Size of layers	2
Number of training trails	6

validation performance was achieved at epoch 0 with an MSE value of $1.8722e^{-06}$. This indicates that the model generalized well to the validation data at the very beginning of training.

The Levenberg-Marquardt approach produced the most accurate overall results ($R=0.99671$). The validation data set’s regression coefficient ($R=1$), indicates a strong connection between ANN and experimental outcomes. Equation 3 calculates the average squared error value.

$$MSE = \frac{1}{n} \sum_{t=1}^n (measured\ value - predicted\ value)^2 \quad (3)$$

Figure 8 illustrates the relationship between the predicted outputs and the actual target values for the training, validation, testing, and overall datasets. Each plot evaluates the model’s accuracy and generalizability for its respective dataset, providing insights into its performance.

Table 6 provides a comparison between the experimental UCS values and those predicted by the ANN model, along with the percentage error for each data point calculated using Equation 4. The results demonstrate a high level of agreement between the experimental and predicted UCS values, as reflected by minimal errors across all cases. In experiment 6, the maximum deviation is observed, with the predicted UCS (44.75 MPa) differing slightly from the experimental value (43.574 MPa), resulting in an error of only 2.699 %, as presented in Figure 9. Overall, the ANN model demonstrates excellent predictive

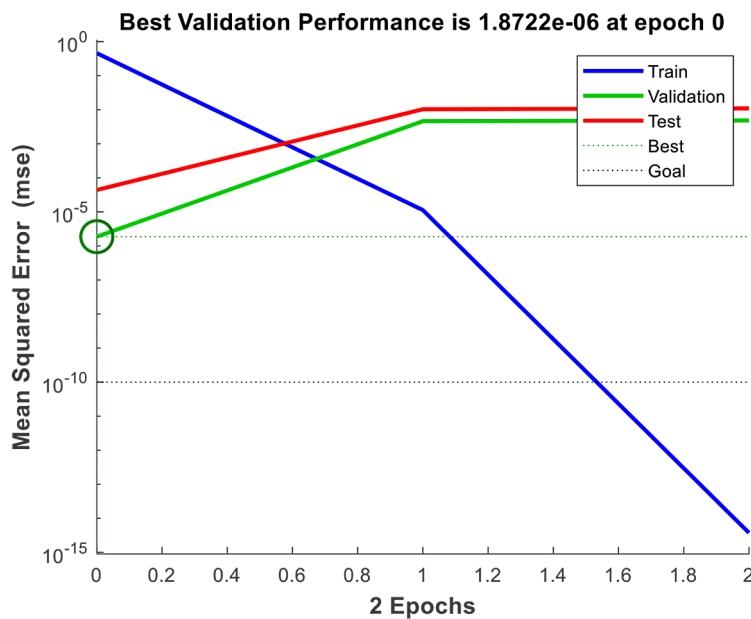


Figure 7. Ultimate compressive strength performance plot

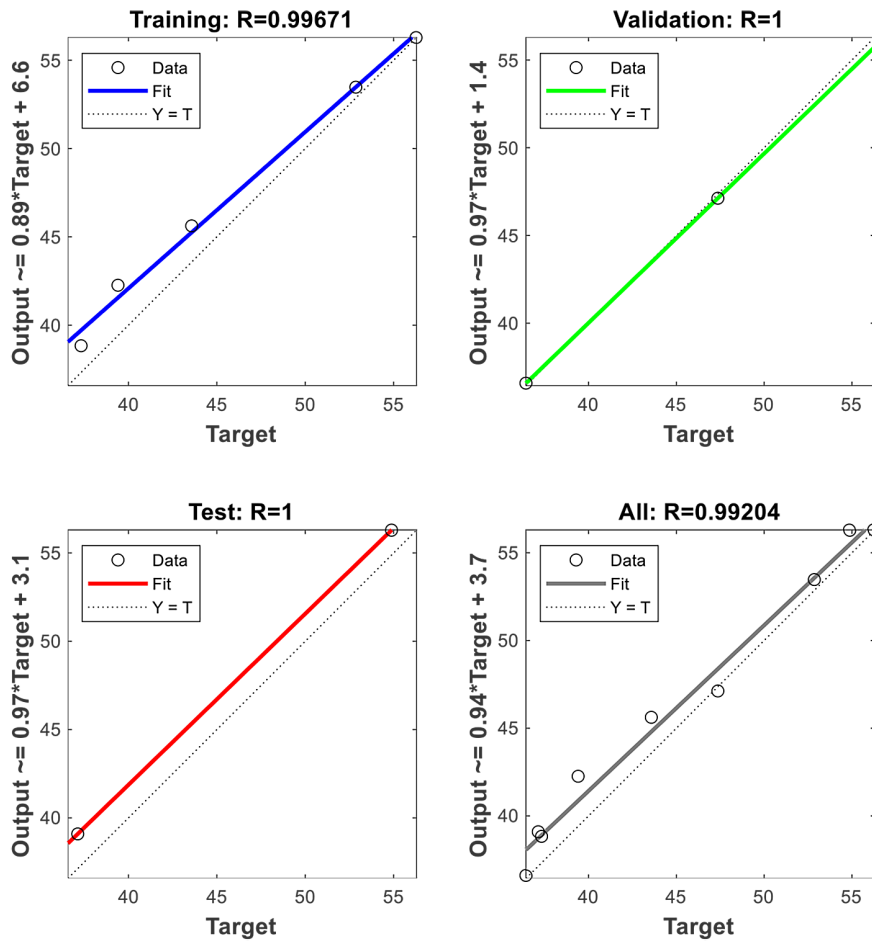


Figure 8. Displays a simplified representation of the suggested system

Table 6. ANN results vs. experimental values for UCS

No.	Experimental UCS	Predicted UCS by ANN	Error %
1	36.438	36.436	0.005
2	37.133	37.13	0.008
3	39.406	39.41	0.010
4	37.322	37.322	0.000
5	47.363	47.35	0.027
6	43.574	44.75	2.699
7	52.858	52.858	0.000
8	56.268	57.621	2.405
9	54.878	54.877	0.002

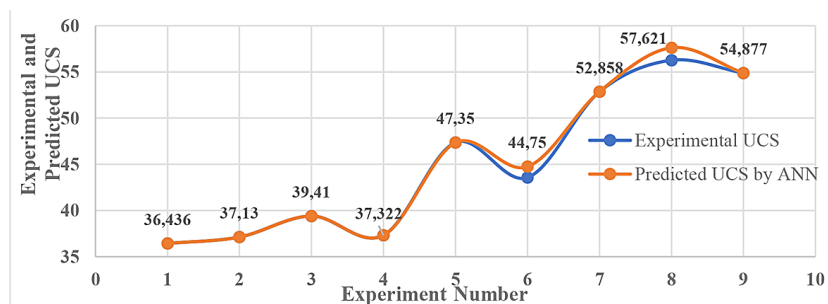


Figure 9. The experimental and predicted compressive strength

accuracy, with errors being negligible in all cases, confirming its reliability for UCS prediction.

$$\text{Error \%} = \left| \left(\frac{\text{measured value} - \text{Predicted value}}{\text{measured value}} \right) \cdot 100 \right| \quad (4)$$

CONCLUSION

This study investigated the effects of FDM 3D printing parameters, which are infill density, infill pattern, and layer thickness, on the UCS of PLA specimens. Using Taguchi's design of experiments, nine experimental runs were conducted, and the UCS results have been analyzed through ANOVA to identify the significance of each parameter. The study revealed the following key findings:

- The highest compressive strength of 56.268 MPa has been achieved using the parameters: Infill Density (80%), Infill Pattern (Gyroid), and Layer Thickness (0.1 mm), while the lowest compressive strength has been observed with the parameters: Infill Density (20%), Infill Pattern (Cubic), and Layer Thickness (0.3 mm).
- The findings revealed that infill density is the most critical factor, contributing 83.56% to the variation in UCS, while infill pattern and layer thickness had minimal effects.
- The optimal parameters for maximizing UCS have been identified as 80% infill density, a gyroid infill pattern, and a 0.3 mm layer thickness based on ANOVA analysis and the Main Effects Plot diagram.
- Additionally, an ANN model has been developed to predict UCS based on the experimental data. The ANN demonstrated excellent predictive accuracy, with a regression coefficient (R) of 0.9974 and minimal errors between experimental and predicted UCS values. The highest error observed was only 2.699%, confirming the reliability of the ANN model for UCS prediction.
- These findings emphasize the importance of selecting appropriate infill density and pattern configurations to enhance the mechanical properties of 3D-printed components. The use of ANN provides an efficient and accurate tool for predicting UCS, which can aid in optimizing FDM processes for various applications requiring high compressive strength.

As mentioned, this work is built on nine data points of experiments. Although it is considered sufficient for the purposes of this study, it is

recommended to use more experimental runs to enhance the reliability of the conclusions. Also, it might uncover other potential trends that are not captured by the current data.

REFERENCES

1. Pietras D., Zbyszyński W., and Sadowski T. A 3D printing method of cement-based FGM composites containing granulated cork, polypropylene fibres, and a polyethylene net interlayer, *Materials*, Jun. 2023; 16(12): 4235, <https://doi.org/10.3390/ma16124235>
2. Fisher T., Almeida Jr J. H. S., Falzon B. G., and Kazancı Z. Tension and compression properties of 3D-printed composites: Print orientation and strain rate effects, *Polymers*, Mar. 2023; 15(7): 1708, <https://doi.org/10.3390/polym15071708>
3. Hossei A. Optimizing print parameters for maximizing tensile strength of additively manufactured polymers through evolutionary algorithms, <https://doi.org/10.7939/r3-e8k0-3291>
4. Ngo T. D., Kashani A., Imbalzano G., Nguyen K. T. Q., and Hui D. Additive manufacturing (3D printing): A review of materials, methods, applications and challenges, *Composites Part B: Engineering*, Jun. 2018; 143: 172–196, <https://doi.org/10.1016/j.compositesb.2018.02.012>
5. Abdulridha H. H., Abbas T. F., and Bedan A. S. Investigate the effect of chemical post processing on the surface roughness of fused deposition modeling printed parts, *Adv. Sci. Technol. Res. J.*, Apr. 2024; 18(2): 47–60, <https://doi.org/10.12913/22998624/183528>
6. Shahrubudin N., Lee T. C., and Ramlan R. An overview on 3D printing technology: Technological, materials, and applications, *Procedia Manufacturing*, 2019; 35: 1286–1296, <https://doi.org/10.1016/j.promfg.2019.06.089>
7. Qin D., Sang L., Zhang Z., Lai S., and Zhao Y. Compression performance and deformation behavior of 3D-printed PLA-based lattice structures, *Polymers*, Mar. 2022; 14(5), 1062, <https://doi.org/10.3390/polym14051062>
8. Chandran V., Kalman J., Fayazbakhsh K., and Bougherara H. A comparative study of the tensile properties of compression molded and 3D printed PLA specimens in dry and water saturated conditions, *J Mech Sci Technol*, May 2021; 35(5): 1977–1985, <https://doi.org/10.1007/s12206-021-0415-5>
9. Brischetto S. and Torre R. Tensile and compressive behavior in the experimental tests for PLA specimens produced via fused deposition modelling technique, *J. Compos. Sci.*, Sep. 2020; 4(3): 140, <https://doi.org/10.3390/jcs4030140>

10. Hamed M. A. and Abbas T. F. The impact of FDM process parameters on the compression strength of 3D printed PLA filaments for dental applications, *Adv. Sci. Technol. Res. J.*, Aug. 2023; 17(4): 121–129, <https://doi.org/10.12913/22998624/169468>
11. Sultana J., Rahman M. M., Wang Y., Ahmed A., and Xiaohu C. Influences of 3D printing parameters on the mechanical properties of wood PLA filament: an experimental analysis by Taguchi method, *Prog Addit Manuf*, Aug. 2024; 9(4): 1239–1251, <https://doi.org/10.1007/s40964-023-00516-6>
12. Farias D., Oliveira D., Quaresma L., Sousa M., Pinheiro M., Angélica R., Da Paz S., Dos Reis M. Effect of infill parameters and nano-reinforcement on compression performance of 3D printed polylactic acid, Feb. 5, 2024, *Chemistry and Materials Science*. <https://doi.org/10.20944/preprints202402.0299.v1>
13. Abdulridha H. H., Abbas T. F., and Bedan A. S. Investigate the effect of chemical post processing on the surface roughness of fused deposition modeling printed parts, *Adv. Sci. Technol. Res. J.*, Apr. 2024; 18(2): 47–60, <https://doi.org/10.12913/22998624/183528>
14. Tunçel O. Optimization of Charpy impact strength of tough PLA samples produced by 3D printing using the Taguchi method, *Polymers*, Feb. 2024; 16(4): 459, <https://doi.org/10.3390/polym16040459>
15. Abdulridha H. H., Abbas T. F., and Bedan A. S. Predicting mechanical strength and optimized parameters in FDM-printed polylactic acid parts via artificial neural networks and desirability analysis, *Management Systems in Production Engineering*, Aug. 2024; 32(3): 428–437, <https://doi.org/10.2478/mspe-2024-0040>
16. Tian Y., Chen C.X., Xu X., et al. A review of 3D printing in dentistry: Technologies, affecting factors, and applications, *Scanning*, Jul. 2021; 2021: 1–19, <https://doi.org/10.1155/2021/9950131>
17. Song Y., Li Y., Song W., Yee K., Lee K.-Y., and Tagarielli V. L. Measurements of the mechanical response of unidirectional 3D-printed PLA, *Materials & Design*, Jun. 2017; 123: 154–164, <https://doi.org/10.1016/j.matdes.2017.03.051>
18. Girish Kumar P. V. R., Devaki Devi K. Optimizing mechanical properties of virgin and recycled PLA components using Anova and neural networks, *Math. models, eng.*, Mar. 2024; 10(1): 1–10, <https://doi.org/10.21595/mme.2023.23630>